Electronic structure of Si(001)-$c(4\times2)$ analyzed by scanning tunneling spectroscopy and *ab initio* simulations

Koji S. Nakayama,[1,2,*] M. M. G. Alemany,[3] Tomoko Sugano,[1,†] Kenji Ohmori,[2,‡] H. Kwak,[4] James R. Chelikowsky,[4] and J. H. Weaver[1,2]

[1]*Department of Materials Science and Engineering and Frederick Seitz Materials Research Laboratory, University of Illinois at Urbana-Champaign, Urbana, Illinois 61801, USA*

[2]*Frederick Seitz Materials Research Laboratory, University of Illinois at Urbana-Champaign, Urbana, Illinois 61801, USA*

[3]*Departamento de Física de la Materia Condensada, Facultad de Física, Universidad de Santiago de Compostela, E-15782 Santiago de Compostela, Spain*

[4]*Departments of Physics and Chemical Engineering, Institute for Computational Engineering and Sciences, University of Texas, Austin, Texas 78712, USA*

(Received 31 March 2005; revised manuscript received 5 December 2005; published 26 January 2006)

We used atomic scale scanning tunneling spectroscopy to map the surface local density of states (LDOS) of clean Si(001)-$c(4\times2)$ at 80 K. Energetically and spatially resolved LDOS images show that the intensity of the controversial 1.4 eV feature in the empty states is high over the troughs between dimer rows and low over the dimers. In contrast, the intensities are inverted in images constructed at 2.1 eV. To understand those results, we undertook *ab initio* calculations using a real-space implementation of density functional theory to obtain contour plots of the surface charge density and the distribution of eigenstates. The simulations demonstrate that the features at 1.4 and 2.1 eV arise from the π^* and σ^* states, respectively, and that π bond interaction between dangling bonds persists in the buckled dimer configuration.

DOI: 10.1103/PhysRevB.73.035330 PACS number(s): 68.37.Ef, 31.15.Ar, 73.20.At

The Si(001) surface has been investigated for decades,[1] and much is known about the clean reconstructed surface, its defects, and changes induced by adsorbates.[2,3] Dimers of the clean Si(001)-(2×1) surface are dynamic at room temperature, with rapid buckling motion that raises one atom and lowers the other. Since the probe speed of the scanning tunneling microscope (STM) is slow compared with the buckling rate, images show what appear to be symmetric dimers. There is a symmetric intermediate state as the dimer switches between extremes, and interactions between two equivalent dangling orbitals give rise to a bonding π band and an antibonding π^* band. Below $\sim$120 K, buckling is quenched,[4] and the dimers are either in phase or out of phase, producing $p(2\times2)$ or $c(4\times2)$ reconstructions.

There have been extensive theoretical and experimental studies of the surface states.[5–16] The surface empty states are important in their own right, but they also play a key role in electronic excitation processes. For example, electron excitations into antibonding levels induce hydrogen desorption,[17] bromine hopping,[18] and the creation of point defects.[19] Recently, Sagisaka *et al.*[20] demonstrated that electron injection into the antibonding surface states of Si(001) could induce a transition between the $p(2\times2)$ and $c(4\times2)$ phases at 4 K. Scanning tunneling spectroscopy (STS) studies of Si(001)-$c(4\times2)$ at low temperature show one filled and three empty state features in local density of states (LDOS) curves.[7,10,13] Throughout this paper, we will use first (−0.4 eV), second ($\sim$0.8 eV), third (1.4 eV), and fourth (2.1 eV) to refer to the order in which the features appear in going from tightly bound filled states to the empty states, where the values in parentheses are obtained in our experiments. There is consensus that the first and the second arise from dimer-derived surface states that extend into the bulk band gap, and we follow the convention of referring to them as π and π^* states instead of the occupied and unoccupied dangling-bonds states introduced by Kröger and Pollmann,[16] who treated the charge transfer from lower to upper atom. The challenge has been to identify the origin of the strong third peak at 1–1.5 eV and the fourth peak at 2.1 eV above the Fermi level (E_F) and to better understand the extent of charge distribution.

For the surface states of Si(001), Kageshima and Tsukada[5] simulated STM images based on linearly combined atomic orbitals. They concluded that the π^* states were dispersive and had lower and upper edges at about +0.3 and +0.9 eV relative to the mid gap for Si(001)-$c(4\times2)$. Northrup[6] also predicted the dispersive nature of the π^* states of Si(001)-$c(4\times2)$, and dispersion was verified by experiments by Yokoyama and Takayanagi[7] and by Okada *et al.*[8] Recently, Kamiński and Jurczyszyn[9] reported density functional calculations for Si(001)-$c(4\times2)$ from which they deduced that the third peak represents the surface band edge formed by π^* states and that those electronic states are mainly localized on the down atoms of a dimer. Based on STS measurements for *n*-type Si(001) at 80 K, Hata *et al.*[10] argued that the third peak at 1.5 eV arose from the dimer σ^* states, which agreed with the interpretation of experiments by Qin and Lagally[11] and with predictions by Krüger *et al.*[12] Most recently, Perdigão *et al.*[13] reported STM and STS measurements for *p*-type Si(001) and concluded that the third peak was mainly caused by backbond states of the up atom of a dimer, which agreed with the interpretation based on room temperature STS by Boland[14] and by Ikegami *et al.*[15]

In this paper, we provide energetically and spatially resolved LDOS maps. Using *ab initio* calculations, we identify the origin of the controversial third and fourth peaks in the

LDOS spectrum of Si(001)-$c(4\times2)$. The LDOS images are important because they can project the spatial distribution of the eigenstates at a given energy, while STM images are mainly constructed from the states between E_F and a given applied bias. The states related to dangling bonds appear at −0.4 and ~0.8 eV from E_F, which is in agreement with a very recent STS study performed on *p*-type Si(001) at 5 K.[13] We show that the states at 1.4 eV are pronounced over the troughs between the dimer rows. At this energy, the LDOS intensity associated with the up atom is slightly higher than that of the down atom. The situation is reversed for the feature at 2.1 eV since the troughs are darker and the dimer rows are brighter. When the surface is saturated with Cl, the peaks at −0.4, ~0.8, and 1.4 eV disappear while the peak at 2.1 eV is enhanced. This is consistent with the third peak arising from dangling-bond derived states. *Ab initio* simulations based on density functional theory show that the 1.4 eV peak arises from π^* states and the structure at ~2.1 eV arises from σ^* states. The simulations also demonstrate incomplete charge transfer from the down to the up atom of a buckled dimer, in contrast to the predictions of Ref. 16. This configuration still allows π bond interaction between the dangling bonds.

The experiments were performed in an ultrahigh vacuum system that has a base pressure of 4×10^{-11} Torr. The samples were *p*-type Si wafers (B-doped, 0.01 Ω cm, Virginia Semiconductor Inc.) that were oriented within 0.5° of (001). Clean Si(001) surfaces were prepared by thermal cleaning in ways that kept the initial defect density below ~1%.[21] The STM tips were tungsten wires (0.38 mm diameter) that were electrochemically etched by KOH and cleaned by electron bombardment in an ultrahigh vacuum. In addition, results were obtained for Cl-saturated Si(001), where the halogens were obtained from an electrochemical cell, as described in detail elsewhere.[22]

Topographic imaging and tunneling spectroscopy was done at 80 K with an Omicron Nanotechnology low temperature STM. For current imaging tunneling spectroscopy[23,24] (CITS), current-voltage (*I-V*) curves were recorded at each pixel of a scanned area while the tunneling gap was fixed by momentarily turning off the feedback loop. A CITS image represents a slice of the three-dimensional database of $I(V,x,y)$ at a given sample bias. A current image can be constructed from a section of $I(V,x,y)$ for any bias, and variations reflect changes in the electronic states accessed. To map the local density of states of the surface, we numerically calculated the normalized tunneling conductance, $(dI/dV)/(I/V)$.

Figure 1(a) is a STM topograph of Si(001)-$c(4\times2)$. Topographs like this represent changes in tip-sample separation when the tunneling current (0.5 nA) is held constant and the tip is scanned across the surface. The image was obtained with electrons tunneling from the sample (biased at −2.0 V) and involved primarily the Si π bonding states. The bright zigzag rows that run diagonally are derived from buckled dimers that form a $c(4\times2)$ pattern. A ball-and-stick model that corresponds to the surface reconstruction is superimposed on the STM image. It shows antiphase ordering of buckled dimers with one atom of a dimer up (large red) and the other down (small blue), with the relative height alternating along the row.

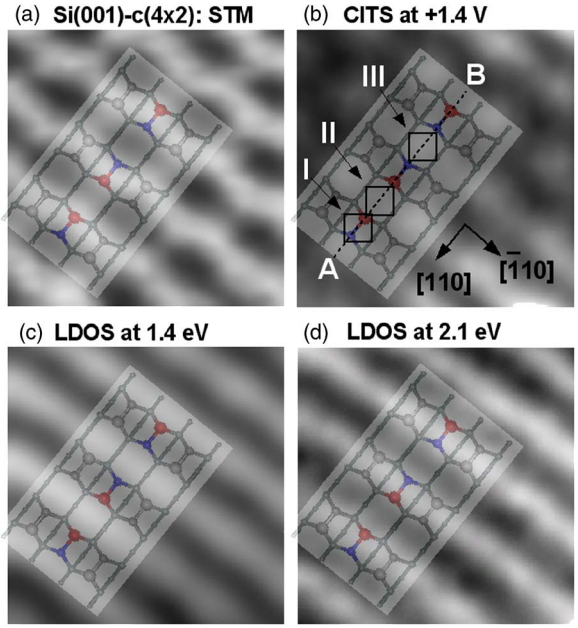

FIG. 1. (Color online) Topographic and spectroscopic features of Si(001)-$c(4\times2)$ acquired at 80 K. In (a), the dimer rows run diagonally and the up atom of a static dimer is bright (occupied-state tunneling, 0.5 nA, sample biased at −2.0 V). Representative positions are identified in a ball-and-stick model that shows antiphase ordering of buckled dimers with one atom up (large red circle) and the other down (small blue circle). Panel (b) is a current image constructed at +1.4 V, where the *I-V* behavior was measured at each pixel with the tip at a fixed height (set at −2.0 V with tunneling current 0.5 nA). Features that were bright in (a) are now dark because of the current was derived from electrons tunneling into empty states within 1.4 eV of E_F. Panel (c) is a LDOS image of the same area constructed at 1.4 eV. It shows a high density of states over the troughs and a low LDOS over the dimers. Panel (d) shows that the situation is reversed in a LDOS image at 2.1 eV because the troughs are dark and the dimers are bright.

The spectroscopic image of Fig. 1(b) was constructed from 125×125 pixels of the 3.1×3.1 nm^2 area of (a). It is an atomic-resolution map of the tunneling current at +1.4 V. The conductance (current) of the down atoms is higher than that of the up atoms (red circles). The center of a dimer has the lowest conductance. The surface contours between (a) and (b) appear inverted because the current in (b) was derived from electrons tunneling into empty states 1.4 eV above the Fermi level rather than from occupied π states which are accessible at −2.0 V sample bias. Line *AB*, which spans the shaded area, is 2.3 nm long and it crosses three dimers along $[\bar{1}\bar{1}0]$. Boxes I–III define positions over a dimer and over the troughs. Each consists of 10×10 pixels. The $(dI/dV)/(I/V)$ spectra in Fig. 2(a) were obtained from these boxes.

Current images contain both geometric and electronic information because the current is derived from the energy integral of the product of the LDOS and the transmission probability, where the latter involves a factor of tip-sample separation.[25,26] To eliminate the transmission factor, we nu-

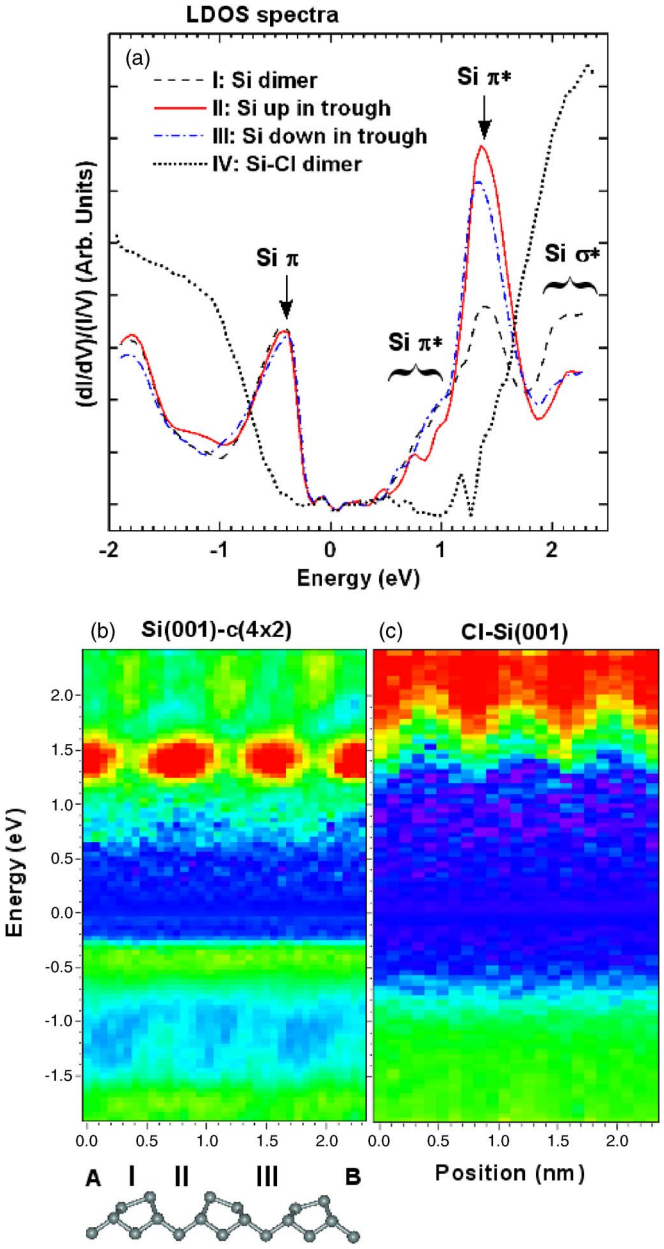

FIG. 2. (Color online) Panel (a) shows representative $(dI/dV)/(I/V)$ spectra taken in squares I–III along line *AB*. IV is taken from Cl saturated Si dimer for comparison with I. Panel (b) is an energetically and spatially resolved LDOS map derived from 35 $(dI/dV)/(I/V)$ spectra measured along *AB*. The buckled dimers are depicted by the ball-and-stick model. The band gap between π and π^* surface states is ~0.7 eV (dark blue central region). The largest conductance (bright red) occurs when the tip is over the trough at 1.4 eV and it is smallest over the dimer. Panel (c) shows the LDOS map for Cl satutated Si(001) that was taken from an equivalent line *AB* in Fig. 1(b). The band gap expands to ~1.7 eV and three states near E_F (zero bias) of (b) disappear, indicating that those states are related to dangling-bond derived states.

merically calculated site by site the normalized differential conductance. Figure 1(c) shows the LDOS at 1.4 eV where the trough conductance is high (cf. site II and III) and the conductance over the dimer is low (cf. site I). There is weak contrast in the trough along the dimer rows in the region between the up atoms (red circles) and the down atoms (blue circles). Figure 1(d) shows that the trough conductance is low and the conductance over the dimer rows is high at 2.1 eV. Thus, the intensity is inverted in comparison with Fig. 1(c). These spatial variations will be discussed below in the context of simulations of the tunneling current.

Figure 2(a) shows representative $(dI/dV)/(I/V)$ spectra taken along line *AB* in Fig. 1. Each was averaged over groups of 10×10 pixels. In agreement with previous interpretations,[1,5–16] the feature at −0.4 V reflects tunneling from π surface states for which there is little intensity variation between dimer and trough. Also in agreement with previous work, we associate the shoulder at ~0.8 eV with tunneling into π^* states. The third feature at 1.4 eV is discussed below. Curves I–III show energetically similar LDOS signatures, though the LDOS intensities of II and III are much higher than that of I at 1.4 eV.

Figure 2(b) is a spatial map of the energy distribution of the LDOS based on 35 spectra like those of Fig. 2(a) along line *AB* (each averaged over 5×5 pixels). The surface band gap is reflected by the deep blue channel separating the π and π^* bands by about 0.7 eV. The Fermi energy lies near the valence band maximum for these boron-doped samples. There are intensity differences along *AB* associated with the π^* states at ~0.8 eV, but the intensity variations associated with the π states at −0.4 eV are smaller, as in (a). The greatest variation occurs at 1.4 eV with high intensity in both trough locations and low intensity over the dimer. From this, the peak at 1.4 eV might appear to reflect σ^* states from Si atoms in the third and fourth layer, which are more accessible over the trough. However, those states decay rapidly with distance from the surface and are unlikely to account for the strongest intensity in the LDOS map.

For electronic states that are related to dangling bonds, we would expect that they disappear if those bonds are saturated with adsorbates. To determine whether the peak at 1.4 eV is derived from dangling bond states rather than σ^* states, we exposed the clean surface to a flux of Cl_2 at room temperature and performed STM/STS measurements on Cl saturated Si(001)-(2×1) at 80 K. The dotted line in Fig. 2(a) shows that all three peaks disappear (at −0.4, ~0.8, and 1.4 eV). Thus, we associate the 1.4 eV peak with dangling-bond derived states. Figure 2(c) shows a LDOS map for the saturated surface taken along a line that is equivalent to *AB*. The surface band gap expands and the intensity over the dimers, where the LDOS had been low for the clean surface, is still low. Instead, the LDOS starts to brighten over the troughs, consistent with the positions of the Cl adatoms and access to the Si-Cl σ^* antibonding levels. Lee and Kang[27] reported first principles calculations for Cl-saturated Si(001) where the Si-Cl σ^* manifold was ~1.6 eV above the valence band maximum, in agreement with experiment. Moreover, the dashed line in Fig. 2(a) shows a broad feature of the bonding states (onset at −0.5 eV and shoulder at about −1.0 eV). This is consistent with the calculations,[27] where states that originate from $p_{x,y}$ orbitals appear below −(0.5–1.5) eV (along Γ-*K*).

In order to clearly identify the electronic states that give rise to the high intensity over the troughs, we carried out

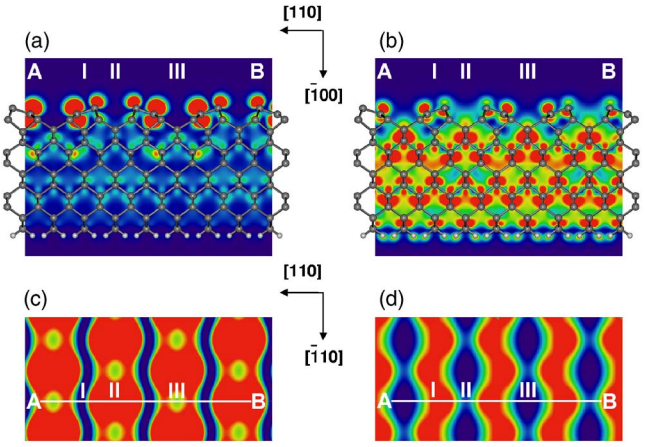

FIG. 3. (Color online) (a) Contour plot of the charge density calculated from Kohn-Sham eigenstates with eigenvalues in the range 1.1 to 1.6 eV on a plane perpendicular to the surface that contains line *AB* in Fig. 1(b). The surface Si atoms have strong intensity (red) because π^* surface states fall in this energy window. (b) The charge density associated with states in the range 1.6 to 2.5 eV, where the bulk Si atoms have strong intensity. (c) The charge density at 0.5 nm from the surface for states with energies between 1.1–1.6 eV. (d) The charge density 0.5 nm away from the surface with states between 1.6–2.5 eV. The maximum intensity represented in (c) and (d) is about four orders of magnitude smaller than that represented in panels (a) and (b). Contour plots correspond to a (8×4) representation of the clean Si(001)-$c(4\times2)$ surface.

ab initio simulations for Si(001)-$c(4\times2)$. The calculations were performed using a real-space implementation of density functional theory, which is based on the self-consistent solution of the one-particle Kohn-Sham equations on a rectangular grid.[28] The electron-ion interation was determined by nonlocal, norm-conserving pseudopotentials generated using the Troullier-Martins prescription.[29] The exchange and correlation potential was described through the local-density functional of Ceperley and Alder.[30] Twelve silicon layers contained in a supercell were considered in the calculations, the lowest of which was passivated by hydrogen atoms. The ground state geometry of the surface was obtained by relaxing the forces acting on atoms as derived from the Hellmann-Feynman theorem.[31] The dimer bond length was 0.229 nm, the tilt angle of the bond was 18.9°, and the two Si atoms were separated by a vertical distance of 0.074 nm. Additional details on the simulation procedure and structural characterization of the surface will be published elsewhere.[32]

Figure 3(a) is a contour plot of the surface charge density associated with eigenvalues in the energy window of 1.1–1.6 eV, which includes the experimental feature at 1.4 eV but not at ~0.8 eV. We define the energy window relative to the experimental energy scale, shifting the calculations by 0.5 eV to account for the underestimation of the band gap due to the local density approximation.[6] Our calculations show three empty states features at 0.2, 0.9, and 1.6 eV above the computational Fermi level.[32] The ball-and-stick model is projected on the charge map. The highest charge density (red) in Fig. 3(a) is around the surface Si atoms, and it arises from the antibonding π combination of the p_z states associated with two surface atoms. These lobed features expand into the vacuum. There is little contribution in this energy window from the bulk states. Thus, the charge density is dominated by states that are limited to the surface. The dimer σ^* states are higher in energy and close to the back bond states and the bulk Si states.[32] We conclude that the charge density in this window corresponds to the π^* surface states. The charge contour has a minimum between two Si atoms, as expected for an antibonding state. The fact that there are empty states associated with both atoms (incomplete charge transfer from lower to up atom) encourages the terminology π-like and π^*-like in discussing the surface states in the buckled configuration. The reconstruction of the surface can still be felt ~5 layers below the surface based on the energy states in the 1.1–1.6 eV window. In contrast, the bulk Si bonds are evident in the 1.6–2.5 eV range, as shown in Fig. 3(b), where strong intensity appeared in the bulk Si bonds and little intensity in the surface dimers. We, therefore, associate the feature that has an onset at about 1.9 eV and a shoulder at 2.1 eV in Fig. 2(a) with Si σ^* states.

To visualize the spatial distribution of the states that expanded into the vacuum, we obtained a contour plot of the charge density 0.5 nm away from the surface.[33] Figure 3(c) shows the spatial distribution of the π^* surface charge along [001] (eigenstate energy window 1.1–1.6 eV). The states are mainly distributed in the troughs where they are evident as red stripes. Those red stripes vary in width as the area probed changes from the trough between two up atoms to the trough between two down atoms. The blue rivers running through the red regions trace the low LDOS of the buckled dimers. Comparison to the experimental result of Fig. 1(c) shows excellent agreement with the undulations of the dark "river." The extent of the high state density along *AB* is similar to the experimentally observed high LDOS region at 1.4 eV, being wider over site II than site III. The low intensity corresponds to the center of the trough between down atoms (III), which corresponds to the dark areas in the occupied state topograph in Fig. 1(a).

We also calculated the empty state charge distribution in the energy window 1.6–2.5 eV. Figure 3(d) shows the results 0.5 nm away from the surface. Now there is a maximum above the dimers (position I) and a minimum over the troughs, in very good agreement with experiment, Fig. 1(d). In contrast, the troughs are bright in STM images taken at +2.0 V sample bias [see, for example, Fig. 1(b) of Ref. 11 and Fig. 6 of Ref. 34]. Since tunneling can involve all states between E_F and the applied bias, the high bias STM images primarily reflect tunneling into the strong states at 1.4 eV. The distinction between STM topographs and LDOS images are important because only the latter can project the eigenstates at a given energy.

In this paper, we showed that STM/STS combined with *ab initio* simulations can be used to map the local density of states of Si(001)-$c(4\times2)$. While STM images are constructed from the states involving them between the Fermi level and a given applied bias, LDOS images can project the states at a given energy. Thus, they can provide the spatial distribution of the eigenstates. The theoretical simulations show the spatial distribution of the eigenstates as a function of energy levels and make it possible to conclude that the strong peak at 1.4 eV corresponds to π^* surface states. The

peak at 2.1 eV arises from σ^* states. This combination of atomic scale spectroscopy and *ab initio* calculations should resolve the controversy in the literature regarding the surface states.[5–16]

This work was supported in part by the National Science Foundation. K.O. was supported by DOE Grant No. DE-FG02-91ER45439 through the Frederick Seitz Materials Research Laboratory. M.M.G.A. acknowledges support from the Spanish Ministry of Education and Science (Program "Ramón y Cajal"), the Spanish Ministry of Education and Science in conjunction with the European Regional Development Fund (Project No. FIS2005-04239), and the Galician Supercomputer Center (CESGA). T.S. acknowledges support from a Japan Patent Office Fellowship. J.R.C. acknowledges support from NSF Grants No. ITR-0082094, DMR-0325218, from DOE under Grants No. DE-FG02-03ER25585, DE-FG02-03ER15491, the National Energy Research Scientific Computing Center, and the Minnesota Supercomputing Institute. We thank R. Butera, A. Agrawal, and A. Signor for stimulating discussions.

*Present address: Institute for Materials Research, Tohoku University, Sendai 980-8577, Japan. Electronic address: kojisn@imr.tohoku.ac.jp

†Permanent address: Japan Patent Office, Kasumigaseki, Tokyo 100-8915, Japan.

‡Present address: National Institute for Materials Science, Nano Materials Laboratory, Ibaraki 305-0044, Japan.

[1] R. J. Hamers, Ph. Avouris, and F. Bozso, Phys. Rev. Lett. **59**, 2071 (1987).

[2] R. S. Becker and R. A. Wolkow, *Scanning Tunneling Microscopy* (Academic Press, New York, 1993), p. 168.

[3] J. A. Kubby and J. J. Boland, Surf. Sci. Rep. **26**, 61 (1996).

[4] R. A. Wolkow, Phys. Rev. Lett. **68**, 2636 (1992).

[5] H. Kageshima and M. Tsukada, Phys. Rev. B **46**, 6928 (1992).

[6] J. E. Northrup, Phys. Rev. B **47**, R10032 (1993).

[7] T. Yokoyama, M. Okamoto, and K. Takayanagi, Phys. Rev. Lett. **81**, 3423 (1998).

[8] H. Okada, Y. Fujimoto, K. Endo, K. Hirose, and Y. Mori, Phys. Rev. B **63**, 195324 (2001).

[9] W. Kaminski and L. Jurczyszyn, Surf. Sci. **566-568**, 29 (2004).

[10] K. Hata, Y. Shibata, and H. Shigekawa, Phys. Rev. B **64**, 235310 (2001).

[11] X. R. Qin and M. G. Lagally, Phys. Rev. B **59**, 7293 (1999).

[12] P. Krüger, A. Mazur, J. Pollmann, and G. Wolfgarten, Phys. Rev. Lett. **57**, 1468 (1986).

[13] L. Perdigão, D. Deresmes, B. Grandidier, M. Dubois, C. Delerue, G. Allan, and D. Stievénard, Phys. Rev. Lett. **92**, 216101 (2004).

[14] J. J. Boland, Phys. Rev. Lett. **67**, 1539 (1991).

[15] H. Ikegami, K. Ohmori, H. Ikeda, H. Iwano, S. Zaima, and Y. Yasuda, Jpn. J. Appl. Phys., Part 1 **35**, 1593 (1996).

[16] P. Krüger and J. Pollmann, Phys. Rev. Lett. **74**, 1155 (1995).

[17] T. C. Shen, C. Wang, G. C. Abeln, J. R. Tucker, J. W. Lyding, Ph. Avouris, and R. E. Walkup, Science **268**, 1590 (1995).

[18] K. S. Nakayama, E. Graugnard, and J. H. Weaver, Phys. Rev. Lett. **89**, 266106 (2002).

[19] K. Nakayama and J. H. Weaver, Phys. Rev. Lett. **82**, 980 (1999).

[20] K. Sagisaka, D. Fujita, and G. Kido, Phys. Rev. Lett. **91**, 146103 (2003).

[21] K. S. Nakayama and J. H. Weaver, Surf. Sci. **574**, 331 (2005).

[22] K. S. Nakayama, E. Graugnard, and J. H. Weaver, Phys. Rev. Lett. **88**, 125508 (2002).

[23] R. J. Hamers, R. M. Tromp, and J. E. Demuth, Phys. Rev. Lett. **56**, 1972 (1986).

[24] A. W. Munz, Ch. Ziegler, and W. Göpel, Phys. Rev. Lett. **74**, 2244 (1995).

[25] R. M. Feenstra, J. A. Stroscio, and A. P. Fein, Surf. Sci. **181**, 295 (1987).

[26] R. M. Feenstra, Phys. Rev. B **60**, 4478 (1999).

[27] J. Y. Lee and M. -H. Kang, Phys. Rev. B **69**, 113307 (2004).

[28] M. M. G. Alemany, M. Jain, L. Kronik, and J. R. Chelikowsky, Phys. Rev. B **69**, 075101 (2004).

[29] N. Troullier and J. L. Martins, Phys. Rev. B **43**, 1993 (1991).

[30] D. M. Ceperley and B. J. Alder, Phys. Rev. Lett. **45**, 566 (1980).

[31] H. Hellmann, *Einführung in die Quantumchemie* (Deuticke, Leipzig, 1937); R. P. Feynman, Phys. Rev. **56**, 340 (1939).

[32] M. M. G. Alemany and J. R. Chelikowsky (unpublished).

[33] According to Ref. 8, the tip-sample distance was ~0.5 nm when the tunneling current was 0.5 nA and the sample bias was −2.0 V. The contour maps were not sensitive to the distance for separations greater than ~0.3 nm.

[34] K. Hata, S. Yasuda, and H. Shigekawa, Phys. Rev. B **60**, 8164 (1999).